might have not only bone health but also compliance advantages for ADT-induced osteoporosis, because the most significant BMD loss occurs within 12 months after ADT therapy in these men.

The findings of the current study demonstrated that urinary NTx returned to the pretreatment levels at the 12-month follow-up in the zoledronate group. If the changes in the urinary NTx levels indicate BMD loss in advance, an annual infusion of zoledronate might be a lower dosage in this patient population, and an infusion every 6 months will be favorable to maintain urinary NTx levels.

Our results are consistent with the results of previously published studies,[10,12] although we evaluated only hormone-naive patients (using zoledronic acid with simultaneous ADT) and consistent timing of follow-up of BMD every 6 months. However, these results do not justify less frequent administration of zoledronic acid to prevent SREs in patients with hormone-naive prostate carcinoma, because the study was powered to demonstrate a significant change in BMD, but was not powered to assess the impact on the risk of SREs.

The prognosis of primary ADT performed in patients with prostate carcinoma is quite good, and 50% of patients were alive after primary ADT at 10-year follow-up in a Japanese population.[3] Thus, we must take care of not only cancer control but also the patient's bone health based on a probably long life span for these men.

Conclusions

A single infusion of zoledronic acid increased BMD and decreased urine NTx levels in hormone-naive patients with prostate carcinoma. These effects were durable within 12 months after the initiation of ADT. However, urinary NTx returned to pretreatment levels at 12 months, and further study is needed to clarify the optimal regimen of therapy, as well as its long-term efficacy.

Conflict of Interest Disclosures

Supported in part by a Grant-in-Aid for Cancer Research from the Ministry of Health, Labor and Welfare, Japan.

References

1. Kawakami J, Cowan JE, Elkin EP, et al. Androgen-deprivation therapy as primary treatment for localized prostate cancer: data from Cancer of the Prostate Strategic Urologic Research Endeavor (CaPSURE). *Cancer.* 2006;106:1708-1714.
2. Shahinian VB, Kuo YF, Freeman JL, et al. Increasing use of gonadotropin-releasing hormone agonists for the treatment of localized prostate carcinoma. *Cancer.* 2005;103:1615-1624.
3. Akaza H. Trends in primary androgen depletion therapy for patients with localized and locally advanced prostate cancer: Japanese perspective [review]. *Cancer Sci.* 2006;97:243-247.
4. Berruti A, Dogliotti L, Terrone C, et al. Changes in bone mineral density, lean body mass and fat content as measured by dual energy x-ray absorptiometry in patients with prostate cancer without apparent bone metastases given androgen deprivation therapy. *J Urol.* 2002;167:2361-2367; discussion 2367.
5. Greenspan SL, Coates P, Sereika SM, et al. Bone loss after initiation of androgen deprivation therapy in patients with prostate cancer. *J Clin Endocrinol Metab.* 2005;90:6410-6417.
6. Shahinian VB, Kuo YF, Freeman JL, Goodwin JS. Risk of fracture after androgen deprivation for prostate cancer. *N Engl J Med.* 2005;352:154-164.
7. Oefelein MG, Ricchiuti V, Conrad W, Resnick MI. Skeletal fractures negatively correlate with overall survival in men with prostate cancer. *J Urol.* 2002;168:1005-1007.
8. Smith MR, Eastham J, Gleason DM, et al. Randomized controlled trial of zoledronic acid to prevent bone loss in men receiving androgen deprivation therapy for nonmetastatic prostate cancer. *J Urol.* 2003;169:2008-2012.
9. Kimura M, Satoh T, Okazaki M, et al. Clinical significance of risedronate for patients with prostate cancer receiving androgen deprivation therapy. *Jpn J Urol.* 2008;99:22-28.
10. Ryan CW, Huo D, Demers LM, et al. Zoledronic acid initiated during the first year of androgen deprivation therapy increases bone mineral density in patients with prostate cancer. *J Urol.* 2006;176:972-978; discussion 978.
11. Israeli RS, Rosenberg SJ, Saltzstein DR, et al. The effect of zoledronic acid on bone mineral density in patients undergoing androgen deprivation therapy. *Clin Genitourin Cancer.* 2007;5:271-277.
12. Michaelson MD, Kaufman DS, Lee H, et al. Randomized controlled trial of annual zoledronic acid to prevent gonadotropin-releasing hormone agonist-induced bone loss in men with prostate cancer. *J Clin Oncol.* 2007;25:1038-1042.
13. Orimo H. Diagnostic criteria of osteoporosis. The Japanese Society for Bone and Mineral Research Consensus Statement 2000. *Osteoporosis Jpn.* 2001;9:9-14.
14. Baim S, Wilson CR, Lewiecki EM, et al. Precision assessment and radiation safety for dual-energy X-ray absorptiometry: position paper of the International Society for Clinical Densitometry. *J Clin Densitom.* 2005;8:371-378.

15. Roach M III, Bae K, Speight J, et al. Short-term neoadjuvant androgen deprivation therapy and external-beam radiotherapy for locally advanced prostate cancer: long-term results of RTOG 8610. *J Clin Oncol.* 2008;26:585-591.

16. D'Amico AV, Denham JW, Bolla M, et al. Short- vs long-term androgen suppression plus external beam radiation therapy and survival in men of advanced age with node-negative high-risk adenocarcinoma of the prostate. *Cancer.* 2007;109:2004-2010.

17. Bolla M, Collette L, Blank L, et al. Long-term results with immediate androgen suppression and external irradiation in patients with locally advanced prostate cancer (an EORTC study): a phase III randomised trial. *Lancet.* 2002;360:103-106.

18. Alibhai SM, Gogov S, Allibhai Z. Long-term side effects of androgen deprivation therapy in men with non-metastatic prostate cancer: a systematic literature review. *Crit Rev Oncol Hematol.* 2006;60:201-215.

19. Groot MT, Boeken Kruger CG, Pelger RC, Uyl-de Groot CA. Costs of prostate cancer, metastatic to the bone, in the Netherlands. *Eur Urol.* 2003;43:226-232.

20. Greenspan SL, Nelson JB, Trump DL, et al. Effect of once-weekly oral alendronate on bone loss in men receiving androgen deprivation therapy for prostate cancer: a randomized trial. *Ann Intern Med.* 2007;146:416-424.

21. Saad F, Gleason DM, Murray R, et al. A randomized, placebo-controlled trial of zoledronic acid in patients with hormone-refractory metastatic prostate carcinoma. *J Natl Cancer Inst.* 2002;94:1458-1468.

The American Journal of Pathology, Vol. 174, No. 6, June 2009

DOI: 10.2353/ajpath.2009.080776

Biomarkers, Genomics, Proteomics, and Gene Regulation

Staphylococcal Nuclease Domain-Containing Protein 1 as a Potential Tissue Marker for Prostate Cancer

Hidetoshi Kuruma,* Yuko Kamata,† Hiroyuki Takahashi,‡ Koji Igarashi,§ Takahiro Kimura,* Kenta Miki,* Jun Miki,* Hiroshi Sasaki,* Norihiro Hayashi,* and Shin Egawa*

From the Departments of Urology, Oncology,† Institute of DNA Medicine, and Pathology,‡ Jikei University School of Medicine, Tokyo, Japan; and the Bioscience Division,§ Reagent Development Department, AIA Research Group, Tosoh Corporation, Kanagawa, Japan*

Using high molecular-weight proteomic analysis, we previously showed that Staphylococcal nuclease domain-containing protein 1 (SND1) is highly expressed in recurrent androgen-insensitive prostate cancer tissues. SND1 is a component of the RNA-induced splicing complex that mediates RNA interference, leading to degradation of specific mRNAs. The objective of this study was to further characterize SND1 expression and to investigate its biological potential in prostate cancer. Radical prostatectomy specimens were obtained from 62 prostate cancer patients. SND1 immunohistochemical staining patterns were evaluated using an in-house polyclonal antibody. We confirmed SND1 mRNA expression in prostate cancer cells using an *in situ* hybridization technique. To determine the importance of SND1 mRNA, we knocked down SND1 *in vitro* with small interfering RNA and observed a significant decrease in cell growth. SND1 was expressed in 60 of 62 prostate cancers (97%), appearing in the cytoplasm as small, granular structures; it was also present at high levels in prostate cancer specimens, while in hyperplasia specimens and normal epithelium, it was weakly or negatively expressed. SND1 expression intensity increased with increasing grade and aggressiveness of the cancer. As SND1 mRNA was overexpressed in cancer cells, the growth of these cells was suppressed following SND1 knockdown *in vitro*, thus representing a promising prostate cancer biomarker and therapeutic target. *(Am J Pathol 2009, 174:2044–2050; DOI: 10.2353/ajpath.2009.080776)*

Prostate cancer is extremely common in Western countries affecting, one in every six men in their lifetime. Most prostate cancers initially require androgen for growth, and thus androgen-depletion therapy leads to marked tumor regression by apoptosis. This therapy is unfortunately only palliative, and some cancer cells develop the ability to proliferate even in the absence of circulating serum androgen. These cells culminate in what is considered an androgen-independent phenotype. We have previously investigated alterations in expression of several proteins in recurrent androgen-dependent prostate cancer LNCaP cells after androgen suppression by proteomic analysis.[1] Staphylococcal nuclease domain-containing protein 1 (SND1), also named Epstein-Barr virus-encoded transcription factor 2 co-activator p100, or Tudor staphylococcal nuclease, was found to exhibit a visually distinct pattern of up-regulation (1.5-fold by densitometric measurement) in androgen-independent cancers, as compared with androgen-dependent cancers in our previous study. This observation prompted us to further investigate the clinical relevance of this particular protein.

SND1 was originally reported in 1995 as a component of the RNA-induced splicing complex that mediates RNA interference in *C. elegans*, leading to degradation of specific mRNA.[2] In mammalian cells, RNA interference occurs subsequent to loading microRNAs (miRs) into RNA-induced splicing complex where they guide mRNA degradation or translation silencing depending on the complementarity of the target.[3] Activation of RNA interference pathway based on miR machinery is very important in oncogenesis and cancer development. Volinia et al[4] reported that miR array of several solid cancers revealed an almost global up-regulation of miRs as a common feature of oncogenesis in many tissue types. Specifically in prostate adenocarcinoma, 39 of 45 differ-

Supported by a Grant-in-Aid from the Ministry of Education, Science, Sports and Culture of Japan, a grant from Japanese Foundation for Prostate Research, the Jikei University Research Found, and Kurozumi Medical Foundation.

Accepted for publication February 17, 2009.

Address reprint requests to Hidetoshi Kuruma, Department of Urology, Jikei University School of Medicine, 3-25-8 Nishi-Shimbashi, Minato-ku, Tokyo, Japan. E-mail: hkuruma@jikei.ac.jp.

ent expressed miRs are up-regulated. An RNase III endonuclease, named dicer, is an essential component of the miR machinery, and its over-expression means activation of RNA interference to degrade target mRNAs. Chiosea et al[5] reported that dicer is up-regulated in prostate cancer. They discussed that dicer may play a role in the early steps of prostate cancer development, probably by potentiating an almost miR up-regulation.

Along with dicer, SND1 is also the central component of the miR machinery. Our previous report revealed SND1 was up-regulated in androgen independent phenotype of prostate cancer. As the one of main player of miR machinery, SND1 may engage early carcinogenesis, and further androgen independency. If it is true, SND1 is likely a marker for prostate cancer and may be used in the detection of the aggressive phenotype. To verify this hypothesis, we validated SND1 expression in surgical specimens and compared its expression pattern and association with histological and clinical parameters in prostate cancer to that α-methylacyl-coenzyme A racemase (AMACR). AMACR is a clinically applicant tissue marker protein, which shows high sensitivity for prostate cancer and is useful for a pathologically doubtful case.[6]

Table 1. Patient Demographics

No. pts.	62
Mean age (range)	65.1 (51–76)
Mean PSA (ng/ml, range)	13.4 (3.69–41.6)
No. PSA (ng/ml) (%)	
<10.0	21 (33.9)
10.0–20.0	29 (46.8)
>20.0	12 (19.4)
No. Gleason score (%)	
2–6	17 (27.4)
7	30 (48.4)
8–10	15 (24.2)
No. highest Gleason pattern (%)	
1	0 (0)
2	7 (11.3)
3	33 (53.2)
4	15 (24.2)
5	7 (11.3)
No. pathological stage (%)	
pT2a	6 (9.7)
pT2b	32 (51.6)
pT3a	19 (30.6)
pT3b	5 (8.1)
No. pos. capsular invasion (%)	21 (33.9)
No. pos. surgical margin (%)	31 (50.0)

No. pts, number of patients, PSA, prostate specific antigen, pos., positive.

Materials and Methods

Patients and Tissue Samples

From 1993 to 2003, 174 patients with prostate cancer received radical retropubic prostatectomy at the Jikei University Hospital. Ninety-three patents received neoadjuvant hormone therapy. Unfortunately, due to the preservation state of some specimens, 21 patients were excluded from this study. Study approval was granted by the Jikei University Ethics Committee Institutional Review Broad.

Table 1 lists characteristics of the patients. Preoperative prostate specific antigen (PSA) was quantified by Tosoh PSA assay (Tosoh Corporation, Tokyo, Japan). Biochemical failure was defined as two consecutive PSA increases ≥0.2 ng/ml. The date of failure was considered to be the time of the first increase.

Morphological Evaluation

All resected specimens were fixed in 10% neutral buffered formalin and embedded in paraffin. Tumors were graded by a single pathologist (H.T.) using the original Gleason grading system.[7] Pathological stage was determined by the same pathologist according to the 2002 TNM classification system.[8] If high-grade prostatic intraepithelial neoplasia (HGPIN) or hyperplasia presented in the same specimen, the corresponding areas were also marked.

Preparation of Polyclonal Antibody to SND1

The antigen peptide RPASPATETVPAFSERTC corresponds to an internal sequence of SND1 (amino acids 423 to 440, Swiss-Prot; *http://br.expasy.org/uniprot/Q7KZF4*). The antigen peptide was conjugated to the carrier protein keyhole limpet hemocyanin and used to immunize *Japanese White* rabbits. The immune response was monitored by enzyme-linked immunosorbent assay and immunoglobulins from high-titer sera were collected with a protein G-immobilized column. The antibody was purified and isolated by affinity purification with a column using immobilized antigen peptide. This antibody was used in the following experiments.

Immunohistochemical Staining

Immunohistochemical (IHC) analysis was performed for the index or largest cancer focus in each surgical specimen. Immunoreactivity of SND1 was compared with that of another commercially available marker, AMACR, for which the rabbit monoclonal antibody P504S (Dako Japan, Tokyo, Japan) was used. Formalin-fixed, paraffin-embedded tissue sections were deparaffinized and rehydrated through a xylene and ethanol series and then treated with 3% hydrogen peroxide for 5 minutes to block endogenous peroxidase activity. Subsequently, slides were washed in distilled water, and then pretreated with citrate buffer solution (pH 6.0) in a microwave at 800 watts power for 10 minutes. After cooling, slides were washed and labeled. Since there was not internal control for adjusting IHC staining, we stained all specimens at the same moment using an automatic staining system; the Ventana Nexus automated stainer with Ventana reagent (Ventana Medical Systems, Inc., Tucson, AZ). The anti-SND1 antibody and P504S were applied at 0.6 mg/ml and a dilution of 1:100, respectively, for 32 minutes at 37°C, and the following detection and visualization procedures were performed according to the manufacture's protocol using the Ventana 3,3-diaminobenzidine

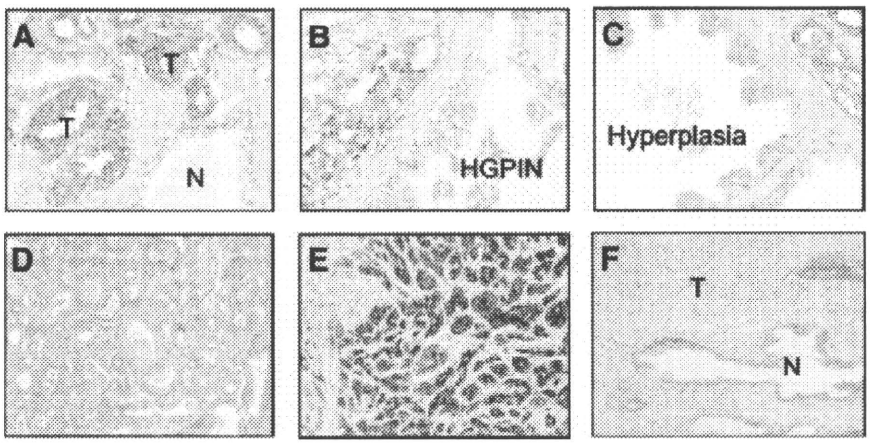

Figure 1. SND1 expression in cancerous prostate tissue. SND1 was localized in the cytoplasm of cancer cells, but not expressed in normal gland (**A**). In HGPIN (**B**) and hyperplasia (**C**), SND1 expression was negative or weakly positive. Cancer of Gleason pattern 2 was stained weakly (**D**), whereas Gleason pattern 5 was stained strongly (**E**). Negative control was not stained both cancer and normal gland (**F**). T: cancer, N: normal gland.

Basic Detection kit (Ventana Medical Systems, Inc.), which includes a universal biotinylated IgG secondary antibody (anti-mouse and anti-rabbit antibodies), avidin horseradish peroxidase, and 3,3-diaminobenzidine. After staining, slides were counterstained with hematoxylin. The specificity of the binding was confirmed by negative staining using rabbit nonimmune serum as a primary antibody.

An IHC score of 1 was assigned for variable or weak cytoplasmic staining, a score of 2 for moderate, apical granular cytoplasmic staining, and a score of 3 for strong cytoplasmic staining. No staining (negative IHC) received a score of 0. The patient's score was the highest score in the index tumor, which was assigned by a single pathologist (H.T.) without access to clinical information. The IHC score was also blindly marked by another independent researcher (H.K.), and then each result was merged. In the case of different score, the two individuals discussed and concluded on a fixed IHC score. Normal area was chosen from an area far from the cancerous area. If the specimen contained HGPIN or hyperplasia lesions, these were evaluated by the same manner.

In Situ *Hybridization*

In situ hybridization of SND1 was conducted as previously described.[9] Complementary DNA was prepared using 1 μg of total RNA isolated from the cell lysate using Isogen (Nippon Gene Co. Ltd, Tokyo, Japan). Primers used to amplify specific gene products were: SND1 forward, 5′-TCATCAAGATGGTCCTCTCA-3′; and SND1 reverse, 5′-CTTAATACGACTCACTATAGGGTGCAATGTTTTCCCCATTGG-3′. The PCR products were obtained using the One-Step reverse transcription (RT)-PCR kit (QIAGEN Japan, Tokyo, Japan) in accordance with the manufacturer's protocol. The PCR product of SND1 was transcribed using a digoxigenin RNA labeling kit (Roche Diagnostics, Basel, Switzerland) to produce a complementary RNA probe. After removing paraffin from paraffin-embedded sections with a xylene and ethanol series, the complementary RNA probe was reacted overnight at 50°C. After a standard blocking treatment, anti-rabbit digoxigenin/horseradish peroxidase antibody (Dako Japan, Kyoto, Japan) was reacted for 15 minutes. The antibody-bound SND1 mRNA was then visualized using the GenPoint System (Dako Japan) in accordance with the manufacturer's protocol.

Cell Lines

The human prostate cancer cell line PC-3 was obtained from the American Type Culture Collection (Rockville, MD). Cells were cultured as a monolayer in Roswell Park Memorial Institute 1640 medium (Invitrogen Japan, Tokyo, Japan) supplemented with 10% fetal bovine serum. Cultures were maintained at 37°C in an atmosphere of humidified air with 5% CO_2.

Small Interfering RNA-Expressing Constructs and Knockdown of SND1

We used small interfering RNAs (siRNAs) predesigned by B-Bridge International (Mountain View, CA) to knock down SND1 mRNA. The target sequences for SND1 are 5′-GGGAGAACACCCAGGATAA-3′ (Si-1) and 5′-CAG-

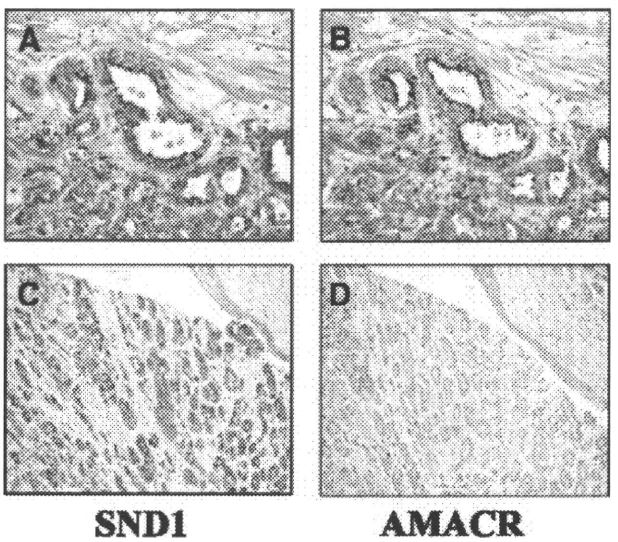

Figure 2. The expressions of SND1 and AMACR in prostate cancer. The expression of AMACR was similar to SND1 (**A, B**), but in some cases, SND1 positive cancer cells (**C**) did not show AMACR expression (**D**).

Table 2. Comparison of IHC Scores between SND1 and AMACR Stratified by Final Diagnosis, PSA, Gleason score, and Pathological Stage for 62 Radical Prostatectomy Specimens

	SND1						AMACR					
IHC score	0	1	2	3	Mean	*P**	0	1	2	3	Mean	*P**
No. cancer total	2	14	40	6	1.8	<0.0001	0	6	25	31	2.4	<0.0001
No. PSA (ng/ml)						0.012						0.85
<10	0	9	10	1	1.6		0	2	9	9	2.4	
10<20	2	5	20	1	1.7		0	2	9	9	2.4	
>20	0	0	9	3	2.3		0	0	6	6	2.5	
No. Gleason score						0.025						0.65
2<6	1	7	9	0	1.5		0	2	8	7	2.3	
7	1	4	23	2	1.9		0	4	10	16	2.4	
8<10	0	3	8	4	2.1		0	0	7	8	2.5	
No. pathological stage						0.95						0.60
pT2	1	8	25	4	1.8		0	4	16	18	2.4	
pT3	1	5	16	2	1.8		0	2	9	13	2.5	
No. HGPIN	7	31	4	0	0.93		4	33	5	0	1.0	
No. hyperplasia	37	14	0	0	0.24		27	24	0	0	0.47	
No. normal gland	47	15	0	0	0.27		34	28	0	0	0.45	

**P* value for differences mean score among groups of cancer, HGPIN, hyperplasia and normal gland, and each group of PSA. Gleason scores were assessed using the Kruskal-Wallis test. *P* value for difference between pT2 and pT3 was assessed using the Mann-Whitney U test.

CAAAGGTCTAGCCACA-3′ (Si-2). PC-3 cells were cultured in a 6-well culture plate at 5×10^5 cells/well. On the following day, the cells were transfected with 0.1 mmol/well of siRNAs using DharmaFECT 2 transfection kit (Dharmacon, Lafayette, CO). As a negative control, cells were treated with an irrelevant siRNA, (5′-ATCCGCGC-GATAGTACGTATT-3′, B-Bridge international). Viable cells were counted 72 hours after transfection. The effect of SDN1 knockdown was expressed as percentage of negative control.

Real-Time Quantitative RT-PCR

Interference with SND1 mRNA expression was confirmed by real-time quantitative RT-PCR, which was performed with TaqMan Gene Expression Assay (Applied BioSystems, Werrington, UK). Total RNA was extracted using the Ambion *mir*Vana PARIS kit (Applied BioSystems). Five-hundred ng of total RNA was used for first-strand cDNA synthesis by SuperScript VILO (Invitrogen, Tokyo, Japan). The cDNA (5 ng of the total RNA) and TaqMan real-time primers and probes were used for amplification. A set of primers and a probe for each gene tested was obtained from Applied Biosystems (SND1 assay ID: Hs00205182-m1, β-actin: TaqMan PreDeveloped Assay Reagents). Fluorescence was detected using the ABI PRISM 7300 sequence detection system (Applied Biosystems). The relative mRNA expression level of each gene for each patient was normalized for input RNA against β-actin expression in the sample.

Statistical Analysis

Clinicopathological parameters were divided into groups; age (<70 or ≥70-year-old), PSA (<10, 10 to 20, or >20 ng/ml), Gleason score (2 to 6, 7, or 8 to 10), and pathological stage (pT2 or pT3). The correlation between SND1 or AMACR expression levels and clinicopathological variables was evaluated using the Mann-Whitney *U* test for comparing between two groups and Kruskal-Wallis test for three or more groups. The probability of biochemical failure was determined using the Kaplan-Meier method. Differences in survival curves were compared using the log-rank test. The Cox proportional hazards regression model was used for multivariate analysis of biochemical

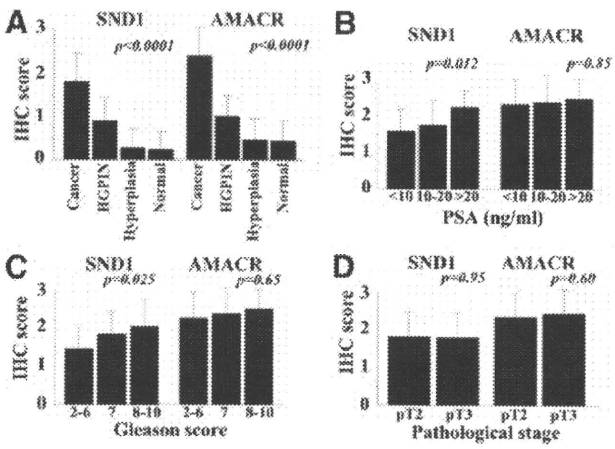

Figure 3. Relative expression of SND1 and AMACR by IHC score stratified by (**A**) histological findings including cancer, HGPIN, hyperplasia and normal glands, (**B**), serum PSA levels, (**C**) Gleason score, and (**D**). pathological stage. Column, mean; bars, SD.

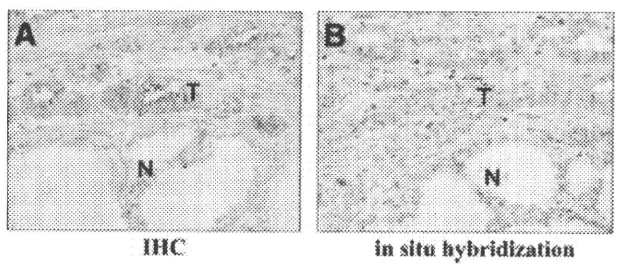

Figure 4. *In situ* hybridization of a surgical specimen for prostate cancer. **A:** IHC shows SND1 was highly expressed in cancer cells (T) but almost negative in noncancerous cell (N). **B:** *In situ* hybridization shows SND1 mRNA was highly expressed in cancer cells (T) but was almost negative or weakly positive in normal luminal cells (N). IHC, immunohistochemistry.

failure risk. Student's *t*-test was used for comparisons of differences between knocked-down cells and negative controls. A difference was considered statistically significant at $P < 0.05$. All analyses were performed with StatView 5.0 statistical package (SAS Institute Inc., Cary, NC) except for Student's *t*-test, which was performed with Excel 2007 software (Microsoft Corporation, Richmond, WA).

Results

IHC Analysis of SND1 and AMACR

IHC staining revealed SND1 predominantly in the cytoplasm of cancer cells, typically as small granular structures (Figure 1A–F). The expression of AMACR was similar, but some SND1-positive cancer cells did not show AMACR expression (Figure 2A–D). In prostate cancer specimen, SND1 and AMACR expression were detected in 60 (97%) and 62 (100%) of a total 62 cases, respectively. However, both SND1 and AMACR were either weakly or not at all expressed (IHC score 0 to 1) in all benign prostatic glands, including the hyperplastic glands and normal luminal cells. In HGPIN, SND1, and AMACR were detected in 83.3% (35/42) and 90.5% (38/42) of the specimens, respectively, though expression was weak in most cases. Overall, order ranked staining from strong to weak appeared as cancer, HGPIN, and benign (Figure 1). The IHC scores in cancer, HGPIN, hyperplasia, and normal luminal cells were 1.7, 0.93, 0.24, and 0.27, ($P < 0.0001$ by Kruskal-Wallis tests) for SND1, respectively, and 1.9, 1.0, 0.47, and 0.45, ($P < 0.0001$ by Kruskal-Wallis tests) for AMACR, respectively (Table 2).

The intensity of SND1 immunoreactivity showed distinct correlation with Gleason score; more intense immunoreactivity being associated with higher specimen score ($p = 0.025$; Figure 3A and C, and Table 2). Expression of SND1 was also associated with high PSA but not with pathological T stage (Figure 3, A, B, and D). By contrast, AMACR showed no relationship with any clinicopathological parameters including Gleason score, PSA level, and pathological T stage.

SND1 mRNA Expression in Tissues

Ten slides were selected randomly for confirmation of SND1 mRNA expression in surgical specimens by *in situ* hybridization. In all selected slides SND1 protein was found positive in cancer cells and negative to weak in expression in normal luminal cells. The intensity of mRNA signals was very similar to the IHC findings. That is, SND1 mRNA was highly expressed in the cytoplasm of cancer cells but was negative to weak in noncancerous cells (Figure 4, A–B).

Knockdown of SND1 by siRNA

Endogenous expression of SND1 mRNA was knocked down by two types of specifically designed siRNAs (Si-1 and Si-2) in the prostate cancer PC-3 cell line. Real-time quantitative RT-PCR showed Si-1 and Si-2 significantly

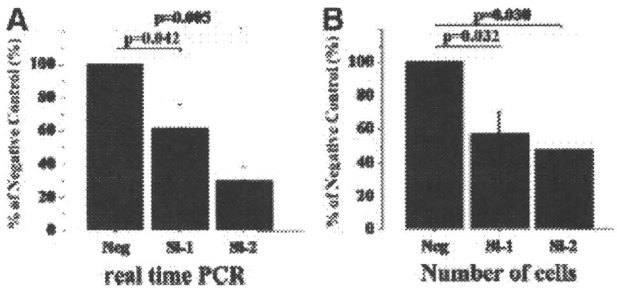

Figure 5. Effect of knockdown of SND1 mRNA in PC-3 cells. **A:** Real-time quantitative RT-PCR showed SND1-specified siRNAs (Si-1, Si-2) significantly decreased SND1 gene expression. **B:** Cell growth of prostate cancer was suppressed comparing to negative control by knockdown with siRNAs. Column, mean; scale bars = SD.

decreased gene expression of SND1, by 62.1% and 30.0%, respectively, compared with the negative control ($p = 0.042$ and 0.005, respectively). In PC-3 cells where SND1 had been knocked down by Si-1 or Si-2 growth was significantly suppressed (by 56.7% and 47.3%, respectively) as compared with control cells, (Figure 5A-B; $p = 0.032$ and 0.030, respectively).

Results of Multivariate Analysis for Biochemical Failure after Surgery

Of 62 patients, 14 were lost during follow-up due to patient noncompliance. No deaths occurred throughout the study. At a median follow-up time from prostatectomy to biochemical failure of 35 months (range, 3 to 113 months) biochemical failure had occurred for 49.1% of these patients. In univariate Kaplan-Meier analysis, primary Gleason grade was associated significantly with biochemical failure ($p = 0.047$). In an exploratory multi-

Table 3. Univariate and Multivariate Analysis (Cox Regression Model) for Biochemical Failure

Variable	HR (95% CI)	*P*
Univariate analysis		
pT stage (≥pT3 vs. <pT3)	1.004 (0.463, 2.175)	0.99
Primary Gleason grade (≥4 vs. <4)	2.184 (1.011, 4.721)	0.047*
Gleason score (≥7 vs. <7)	2.493 (0.926, 6.712)	0.071
Capsular invasion (positive versus negative)	1.425 (0.654, 3.107)	0.37
SND1 IHC score (≥2 vs. <2)	1.627 (0.612, 4.325)	0.33
AMACR IHC score (≥3 vs. 3)	0.761 (0.348, 1.660)	0.49
Multivariate analysis		
pT stage (≥pT3 vs. <pT3)	0.283 (0.089, 0.904)	0.033*
Capsular invasion (positive versus negative)	3.324 (1.031,10.139)	0.044*
SND1 IHC score (≥2 vs. <2)	2.228 (0.643, 7.717)	0.21
AMACR IHC score (≥3 vs. 3)	0.391 (0.144, 1.059)	0.065

*$P < 0.05$.

variate analysis that included age, PSA, pathological stage, capsular invasion, surgical margin, primary Gleason grade, SND1 intensity, and AMACR intensity, pathological stage and capsular invasion SND1 had independent prognostic significance. However, high SND1 expression was not an independent predictor for biochemical failure after radical prostatectomy ($p = 0.21$, Table 3).

Discussion

We have shown evidence for the diagnostic potential of SND1 in prostate surgical specimens equivalent or better than that of AMACR. There have been numerous reports indicating the effectiveness of AMACR for identifying cancer, which have resulted to its use in the clinical setting.[10] However, since AMACR staining is unstable and the test shows unsatisfactory specificity, it is considered insufficient for use as an independent tumor diagnostic marker. In cases with difficult pathological diagnosis, an antibody cocktail containing AMACR together with the basal cell markers 34βE12 and p63 is available for cancer confirmation.[11] SND1 offers a promising new tissue marker, however its specificity, although better than that of AMACR, is still not sufficient for use as a sole marker. SND1 and AMACR do show different expression in some cases (Figure 2, C–D) and therefore the possibility of SND1 joining the cocktail of pathologically useful tissue markers that includes AMACR, 34βE12, and p63 is favored.

At this time, the Gleason score of biopsy specimens is the most powerful predictor of prostate cancer progression, and is an essential parameter in nomograms for predicting clinically insignificant cancer.[12] However, since the Gleason grading system is based solely on glandular architecture, small specimens such as needle biopsy samples often show poor interpathologist reproducibility.[13] Moreover, scores are based on the pathologist's subjective impression and experience. Even in surgical specimens, the scores assigned by trained observers disagree with those previously assigned in over 70% of cases.[14] Hence, a new tissue marker that reflects grade of malignancy would contribute significantly to the objective assessment of prostate cancer. We found that prostate cancer cells with higher Gleason score exhibited more intense SND1 expression than did those with lower grades (Figure 3, A and C). It seems reasonable to suppose that SND1 is related with aggressiveness of prostate cancer. To put in clinical language, although some of Gleason 8 to 10 cancers only showed weak expression, SND1 may offer an important role in distinguishing the presence of a more aggressive and clinically significant phenotype. In our study, statistical significance was not observed through multivariate analysis to identify high SND1 expression as an independent predictor of biochemical failure after radical prostatectomy, and this may be attributed to the small sample size used. Since statistical significance was also not found for specimen Gleason score in this study, the small sample size may have contributed to this overall observation of SND1 not being an independent predictor of biochemical failure. Follow-up studies with a larger sample population are necessary to investigate this.

siRNAs specifically knocked down SND1 mRNA and effectively inhibited cell proliferation of PC-3 prostate cancer cells (Figure 5). Reports of this molecule's function in other settings have recently appeared and may provide insight as to its function in prostate cancer cells. SND1 was previously identified as an enhancer of the transcription activity of Epstein-Barr virus nuclear antigen 2 and also as a protein that is essential for normal growth of B lymphocytes.[2] SND1 has four staphylococcal nuclease-like domains (SN-like domains) and a Tudor domain.[15] It has been demonstrated to bind with signal transducer and activator of transcription 6 via an SN-like domain, to bind with the large fragment of RNA polymerase II, and to control the basal transcription mechanism of signal transducer and activator of transcription 6 by a bridging function.[16] In addition, SND1 binds to c-Myb, a differentiation and growth factor of immature hematopoietic cells and lymphocytes, suggesting involvement in up-regulation of translation.[17] Although SND1 is located primarily in the cytoplasm, it can also migrate to the nucleus and has been indicated as possessing the potential to control translation activity.[18] Tsuchiya et al[19] reported the involvement of SND1 in colon carcinogenesis, with SND1 suppressing the adenomatous polyposis coli protein level via a post-transcriptional mechanism. These authors found no relation to tumor aggressiveness or progression, leading them to suggest possible involvement of SND1 in early-stage carcinogenesis in colon cancer. In prostate cancer, although SND1 could contribute to the RNA degradation observed in RNA interference, the target RNA has not been defined. However, many miRs were up-regulated in prostate cancer, and targets of these miRs include major tumor suppressor genes. For example, let-7 negatively regulates Ras, miR-17-5p, and miR-20a control E2F, and miR-16-1 and miR-15a repress Bcl-2.[5] Since the miR machinery including engagement of SND1 in prostate cancer is somewhat of a black box, further studies are warranted.

In conclusion, SND1 may have the potential for identification of the more aggressive and clinically significant prostate cancers.

Acknowledgments

We thank William A. Thomasson, Ph.D. and Ms. Jennifer Locke for expert editorial assistance.

References

1. Kuruma H, Egawa S, Oh-Ishi M, Kodera Y, Satoh M, Chen W, Okusa H, Matsumoto K, Maeda T, Baba S: High molecular mass proteome of androgen-independent prostate cancer. Proteomics 2005, 5:1097–1112
2. Tong X, Drapkin R, Yalamanchili R, Mosialos G, Kieff E: The Epstein-Barr virus nuclear protein 2 acidic domain forms a complex with a novel cellular coactivator that can interact with TFIIE. Mol Cell Biol 1995, 15:4735–4744
3. Bernstein E, Caudy AA, Hammond SM, Hannon GJ: Role for a bidentate ribonuclease in the initiation step of RNA interference. Nature 2001, 409:363–366

4. Volinia S, Calin GA, Liu CG, Ambs S, Cimmino A, Petrocca F, Visone R, Iorio M, Roldo C, Ferracin M, Prueitt RL, Yanaihara N, Lanza G, Scarpa A, Vecchione A, Negrini M, Harris CC, Croce CM: A microRNA expression signature of human solid tumors defines cancer gene targets. Proc Natl Acad Sci USA 2006, 103:2257–2261
5. Chiosea S, Jelezcova E, Chandran U, Acquafondata M, McHale T, Sobol RW, Dhir R: Up-regulation of dicer, a component of the MicroRNA machinery, in prostate adenocarcinoma. Am J Pathol 2006, 169:1812–1820
6. Magi-Galluzzi C, Luo J, Isaacs WB, Hicks JL, de Marzo AM, Epstein JI: Alpha-methylacyl-CoA racemase: a variably sensitive immunohistochemical marker for the diagnosis of small prostate cancer foci on needle biopsy. Am J Surg Pathol 2003, 27:1128–1133
7. Gleason DF: Classification of prostatic carcinomas. Cancer Chemother Rep 1966, 50:125–128
8. UICC International Union: UICC International Union Against Cancer, TNM classification of malignant tumors, 6th ed. Edited by Sobin LH, Wittekind CH. New York, John Wiley & Sons, Inc, 2002, pp. 184–187
9. Tsuchiya B, Sato Y, Montone KT, Nagai T, Kameya T: Four-hour double staining for in situ hybridization and immunohistochemistry. The J Histotechnol 2000, 23:321–325
10. Rubin MA, Zhou M, Dhanasekaran SM, Varambally S, Barrette TR, Sanda MG, Pienta KJ, Ghosh D, Chinnaiyan AM: alpha-Methylacyl coenzyme A racemase as a tissue biomarker for prostate cancer. JAMA 2002, 287:1662–1670
11. Humphrey PA: Diagnosis of adenocarcinoma in prostate needle biopsy tissue. J Clin Pathol 2007, 60:35–42
12. Epstein JI, Partin AW, Sauvageot J, Walsh PC: Prediction of progression following radical prostatectomy. A multivariate analysis of 721 men with long-term follow-up Am J Surg Pathol 1996, 20:286–292
13. Steinberg DM, Sauvageot J, Piantadosi S, Epstein JI: Correlation of prostate needle biopsy and radical prostatectomy Gleason grade in academic and community settings. Am J Surg Pathol 1997, 21:566–576
14. Montironi R, Mazzucchelli R, Scarpelli M, Lopez-Beltran A, Fellegara G, Algaba F: Gleason grading of prostate cancer in needle biopsies or radical prostatectomy specimens: contemporary approach, current clinical significance and sources of pathology discrepancies. BJU Int 2005, 95:1146–1152
15. Callebaut I, Mornon JP: The human EBNA-2 coactivator p100: multidomain organization and relationship to the staphylococcal nuclease fold and to the tudor protein involved in Drosophila melanogaster development. Biochem J 1997, 321:125–132
16. Yang J, Aittomäki S, Pesu M, Carter K, Saarinen J, Kalkkinen N, Kieff E, Silvennoinen O: Identification of p100 as a coactivator for STAT6 that bridges STAT6 with RNA polymerase II. EMBO J 2002, 21:4950–4958
17. Leverson JD, Koskinen PJ, Orrico FC, Rainio EM, Jalkanen KJ, Dash AB, Eisenman RN, Ness SA: Pim-1 kinase and p100 cooperate to enhance c-Myb activity. Mol Cell 1998, 2:417–425
18. Ness SA: Myb binding proteins: regulators and cohorts in transformation. Oncogene 1999, 18:3039–3046
19. Tsuchiya N, Ochiai M, Nakashima K, Ubagai T, Sugimura T, Nakagama H: SND1, a component of RNA-induced silencing complex, is up-regulated in human colon cancers and implicated in early stage colon carcinogenesis. Cancer Res 2007, 67:9568–9576

BJUI
BJU INTERNATIONAL

Characterization of the anatomical extension pattern of localized prostate cancer arising in the peripheral zone

Mototsugu Muramaki, Hideaki Miyake, Toshifumi Kurahashi, Atsushi Takenaka and Masato Fujisawa

Division of Urology, Kobe University Graduate School of Medicine, Kobe, Japan

Accepted for publication 8 July 2009

Study Type – Diagnostic (non-consecutive series)
Level of Evidence 3b

OBJECTIVES

To characterize the anatomical extension pattern of prostate cancer arising in the peripheral zone (PZ) in radical prostatectomy (RP) specimens and to evaluate its prognostic significance.

PATIENTS AND METHODS

Of 174 consecutive patients undergoing RP, 128 diagnosed as having PZ cancer (PZC) were enrolled. The maximum tumour area (MTA) and maximum tumour volume (MTV) in RP specimens were measured using digital planimetry. A circle with an area equal to the MTA, in which the central point was the intersection of the longest line of the MTA and the line perpendicularly bisecting the first line, was defined as a hypothetical extension area, regardless of anatomical structure. The area within this circle that did not overlap the MTA was defined as ΔTA.

RESULTS

There was a significant correlation between the MTV and ΔTA/MTA, introduced as a variable representing the degree of PZC extension along the anatomical shape of the PZ. The ΔTA/MTA in patients with a MTV of >5 mL was significantly greater than that in those with a MTV of ≤5 mL. Furthermore, ΔTA/MTA was significantly associated with several prognostic indicators, including extracapsular extension, surgical margin status and perineural invasion. Multivariate analysis identified ΔTA/MTA in addition to preoperative serum prostate-specific antigen level, extracapsular extension and surgical margin status as independent predictors of biochemical recurrence after RP.

CONCLUSIONS

PZC tends to extend along the anatomical shape of the PZ during progression, resulting in higher ΔTA/MTA value in advanced PZC than that in early PZC.

KEYWORDS

prostate cancer, radical prostatectomy, peripheral zone, biochemical recurrence

INTRODUCTION

Since McNeal [1] first described three different anatomical zones in the human prostate, several investigators have evaluated the characteristics of prostate cancer according to the zonal origin [2–4] The peripheral zone (PZ) is the predominant location of the origin of prostate cancer, and the proximity of these cancers to the rectal surface can facilitate the diagnosis by palpation and needle biopsy, while prostate cancers arising in the transition zone (TZ) are frequently found incidentally in TURP specimens [5]. Interestingly, despite higher serum PSA levels and tumour volumes, TZ cancer (TZC) more frequently shows favourable pathological findings and better biochemical cure rate after radical prostatectomy (RP) than PZ cancer (PZC) [2–4]. Furthermore, several recent studies have reported that PZC might have more aggressive biological features than TZC [6,7]. Collectively, these findings suggest that it would be suitable to consider PZC and TZC as diseases having different malignant phenotypes.

Despite the intensive efforts investigating differences in the clinicopathological characteristic between PZC and TZC [2–7], there have been few studies systematically analysing the extension pattern of each disease within the prostate gland. In our previous study evaluating the effect of the location of positive biopsy cores on the findings of RP specimens, locally advanced prostate cancers were shown to frequently involve the anterior lateral horn, representing the extreme lateral and anterior PZ that surrounds the TZ, although whether cancer was detected in the ALH or other areas does not seem to affect the biological features [8]. In that study, we also found that tumours detected from the anterior lateral horn had an incidence of TZ involvement similar to that detected from other anatomical sites [8]. These findings suggest that tumours derived from the PZ seem to spread through the PZ and/or across the capsule, but not through the TZ. In the present study therefore, we precisely analysed the RP specimens obtained from patients diagnosed as having disease arising from the PZ, to clarify the extension pattern of PZC and to determine its prognostic significance in patients undergoing RP.

FIG. 1. Schematic presentation of the whole-mount section of a RP specimen. The MTA of the largest single tumour focus was determined using digital planimetry. Line AA' and BB' is the longest line in the MTA and the line perpendicularly bisecting AA', respectively. The circle has the same area as the MTA, and the central point is the intersection of AA' and BB'. The area within this circle that did not overlap the MTA was measured and defined as ΔTA. Solid line, prostate capsule; broken line, boundary of PZ and TZ.

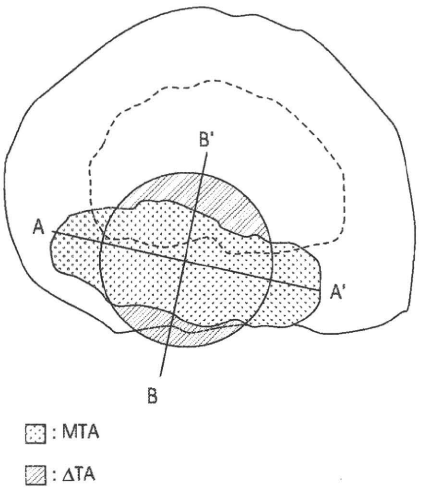

TABLE 1 The characteristics of 128 patients who had RP for PZC

Variable	Median (range) or *n* (%)
Age, years	67.5 (50–78)
Pathological stage	
pT2	91 (71.1)
pT3a	19 (14.8)
pT3b	18 (14.1)
PSA level, ng/mL	9.5 (2.8–6.2)
Gleason score	
≤6	24 (18.7)
3 + 4	44 (34.4)
4 + 3	55 (43.0)
≥8	5 (3.9)
Lymph node metastasis	
Negative	128 (100.0)
Positive	0
SMS	
Negative	97 (75.8)
Positive	31 (24.2)
Lymphatic invasion	
Negative	100 (78.1)
Positive	28 (21.9)
Vascular invasion	
Negative	91 (71.1)
Positive	37 (28.9)
PNI	
Negative	21 (16.4
Positive	107 (83.6)

PATIENTS AND METHODS

The study included 174 patients who were diagnosed as having clinically organ-confined prostate cancer according to the staging procedures used at our institution, including a DRE, TRUS, serum PSA assay, pelvic CT, MRI and/or a bone scan. The patients subsequently had RP and bilateral pelvic lymphadenectomy, based on the surgical procedure described by Walsh *et al.* [9], between May 2003 and December 2007m with no neoadjuvant therapy. The median (range) follow-up of the patients was 44.3 (13–67) months. Informed consent for the current study using RP specimens was obtained from each of the patients, and the study design was approved by the Research Ethics Committee of our institution.

RP specimens were prepared by the whole-mount technique, the surface was inked, and the specimen fixed in 10% neutral formalin. After fixation, the apex and base were cut off and serially sectioned along the vertical parasagittal plane. The seminal vesicles were sectioned parallel to their junction with the prostate and submitted entirely for evaluation. The remaining specimen was serially sectioned perpendicularly to the long axis of the gland from the apex to the base at ≈5-mm intervals. All sections were processed with haematoxylin and eosin on slides for microscopic evaluation.

In this series, the samples were examined pathologically by one pathologist according to the 2002 TNM classification system. Surgical margins were diagnosed as positive if the cancer cells reached the inked margin at any location in the RP specimen.

After RP patients were followed by periodic measurement of serum PSA levels at least every 3 months for the first 2 years, and every 6 months thereafter. Biochemical recurrence was defined as a PSA level persistently >0.2 ng/mL. Irrespective of pathological findings suggesting a poor prognosis, none of the patients received any adjuvant therapy until their serum PSA levels reached ≥0.4 ng/mL.

All tumour areas were marked on whole-mount slides with a water-resistant pen. The maximum tumour area (MTA) of the largest single tumour focus was determined using a digital planimeter (Uchida Yoko, Tokyo, Japan), and the maximum tumour volume (MTV) was calculated as the sum of surface areas for that tumour multiplied by the thickness of the prostate slice as previously described [7]. The MTA and the MTV *in vivo* were corrected for tissue shrinkage during formalin fixation by multiplying by a factor of 1.21 and 1.33, respectively. The boundary between PZ and TZ is marked by a stromal band that is nearly devoid of glandular elements. TZC was considered when >70% of the cancer area was located in the TZ, while the remaining cases were defined as PZC.

To characterize the extension pattern of PZC using an objective method we used a new variable calculated as described below. As shown in Fig. 1, we drew a circle with an area equal to MTA, in which the central point was the intersection of the longest line in the MTA (AA') and a line perpendicularly bisecting AA' (BB'). This was defined as the hypothetical extension pattern regardless of anatomical structure. The area within this circle that did not overlap MTA was measured and defined as ΔTA. Finally, the ΔTA/MTA value was calculated by dividing ΔTA by MTA.

The variables for different groups were compared statistically using the Mann-Whitney *U*-test and chi-square test. Survival curves were compared using the Kaplan-Meier method and analysed by log-rank tests. Cox proportional hazards models were used to assess the hazard ratio with 95% CI, under univariate and multivariate analyses. In all tests $P < 0.05$ was considered to indicate significance.

RESULTS

According to the definition described above, 128 of 174 patients were diagnosed as having PZC and were further analysed to evaluate the extension pattern of PZC within the prostate gland. The clinicopathological characteristics of these 128 patients are summarized in Table 1.

The median (range) values of MTA, MTV, ΔTA and ΔTA/MTA in the 128 patients with PZC were 1.79 (0.15–14.64) cm^2, 1.86

FIG. 2. Correlation between MTV and ΔTA/MTA in RP specimens from 128 patients with PZC.

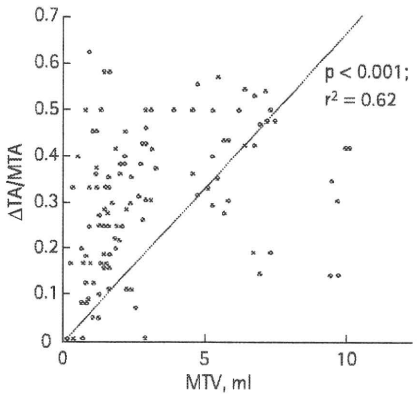

FIG. 3. A comparison of PZ and TZ ΔTA/MTA values according to MTV in RP specimens from 128 patients with PZC.

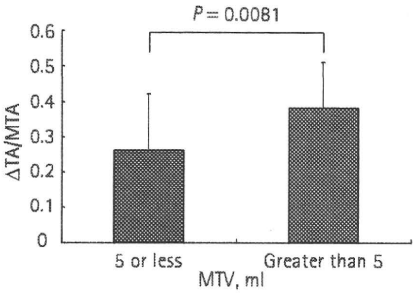

TABLE 2 The association between ΔTA/MTA and clinicopathological factors in 128 patients who had RP for PZC

Variables	ΔTA/MTA ≤30	ΔTA/MTA >30	*P*
N	60	68	
Age, years			
≤65	29	35	0.720
>65	31	33	
PSA level, ng/mL			
≤10	28	36	0.530
>10	32	32	
ECE			
Negative	51	40	0.011
Positive	9	28	
SVI			
Negative	54	56	0.210
Positive	6	12	
Gleason score			
3 + 4, ≤6	33	35	0.690
4 + 3, ≥8	27	33	
SMS			
Negative	51	46	0.022
Positive	9	22	
Lymphatic invasion			
Negative	46	54	0.710
Positive	14	14	
Vascular invasion			
Negative	40	51	0.300
Positive	20	17	
PNI			
Negative	16	5	0.032
Positive	44	63	

TABLE 3 Univariate and multivariate analyses of several variables as predictors of biochemical recurrence after RP

Variable	Hazard ratio (95% CI), *P* Univariate	Multivariate
Age, years (≤65 vs >65)	1.30 (0.44–1.74), 0.610	1.25 (0.51–1.38), 0.730
PSA level, ng/mL (≤10 vs >10)	3.24 (1.22–3.98), 0.025	3.51 (1.17–4.32), 0.022
ECE (–ve vs +ve)	3.87 (1.47–5.35), 0.043	4.17 (2.11–5.80), 0.032
SVI (–ve vs +ve)	4.17 (1.87–7.10), 0.010	5.22 (1.57–9.46), 0.008
Gleason score (3 + 4, ≤6 vs 4 + 3, ≥8)	1.33 (0.91–2.87), 0.370	1.28 (0.54–2.87), 0.210
SMS (–ve vs +ve)	2.97 (1.17–5.41), 0.009	3.94 (1.18–4.81), 0.010
Lymphatic invasion (–ve vs +ve)	1.28 (0.43–3.02), 0.540	1.47 (0.33–2.45), 0.260
Vascular invasion (–ve vs +ve)	1.54 (0.71–3.64), 0.320	0.89 (0.25–1.32), 0.540
PNI (–ve vs +ve)	1.59 (0.75–2.95), 0.460	1.41 (1.65–3.98), 0.360
ΔTA/MTA (≤30 vs >30)	2.41 (1.28–6.41), 0.031	2.88 (1.22–6.33), 0.042

(0.090–10.11) cm^3, 0.48 (0–3.59) cm^2 and 0.30 (0–0.63), respectively. We initially assessed the relationship between MTV and ΔTA/MTA values in these 128 patients; there was a significant linear relation with MTV values (Fig. 2). Furthermore, when the 128 patients were divided into two groups according to the value of MTV, the ΔTA/MTA value in patients with a MTV of >5 mL was significantly greater than that in those with a MTV of ≤5 mL (Fig. 3). The association between ΔTA/MTA and several clinicopathological variables was then evaluated (Table 2); the ΔTA/MTA was significantly associated with extracapsular extension (ECE), surgical margin status (SMS) and perineural invasion (PNI), but there were no significant relations between ΔTA/MTA and the remaining factors, including age, preoperative serum PSA level, seminal vesicle invasion (SVI), Gleason score, lymphatic invasion and vascular invasion.

FIG. 4. Biochemical recurrence-free survival of 128 patients with PZC who had RP, according to ΔTA/MTA values.

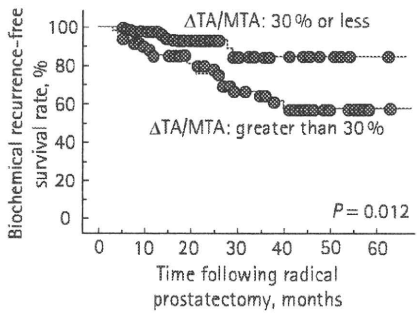

During the observation period of the study, 26 of the 128 patients had a biochemical recurrence after RP. The effect of ΔTA/MTA on biochemical recurrence after RP in the 128 patients with PZC was investigated using univariate and multivariate analyses (Table 3). The univariate analysis identified ΔTA/MTA value in addition to preoperative serum PSA level, ECE, SVI and SMS as significant predictors of the biochemical outcomes. In addition, these five variables, including ΔTA/MTA, were independently associated with biochemical recurrence on multivariate analysis. There was a significant difference in the biochemical recurrence-free survival in the 128 patients according to ΔTA/MTA value (Fig. 4).

DISCUSSION

Prostate cancer arising in the TZ has been shown to have several characteristics differing from those of tumour arising in the PZ [2–5]. Of these, the most important difference is that TZC might have less aggressive features than PZC, although TZC is

characterized by obviously high serum PSA value and a greater tumour volume than PZC [2–4]. Furthermore, several studies analysing morphological, genetic and biological differences between TZC and PZC were reported recently [6,7]. These findings suggest a potential effect of zonal origin on the phenotype of prostate cancer; accordingly, it would be of interest to assess the extension pattern of prostate cancer in the prostate and its relation to conventional clinicopathological variables.

To date, there have been few studies quantitatively addressing the extension pattern of prostate cancer; hence, in the present study we introduced a new variable, ΔTA/MTA, representing the extension pattern of prostate cancer arising in the PZ, to objectively evaluate its significance. It was initially hypothesized that if prostate cancer arising in the PZ progresses regardless of any anatomical limitations, including the prostate capsule and the boundary between PZ and TZ, these tumours would extend concentrically from the centre of the tumour. Based on this notion, a measurement of the tumour volume that does not overlap either the real tumour shape or the virtual sphere with an identical centre and sharing the same volume as the real tumour, might represent how this tumour progresses along the anatomical shape of the PZ. Furthermore, the measurement of this volume could be reasonably substituted by measuring the tumour areas in the section at MTA; therefore, we introduced ΔTA/MTA value as a variable reflecting the extension pattern of PZC.

In this series of 128 patients diagnosed as having PZC, the ΔTA/MTA value had a linear correlation with the MTV. This outcome strongly suggests that PZC might extend along the anatomical shape of the PZ in the prostate. However, some cases with a large MTV had a comparatively low ΔTA/MTA. This phenomenon could be explained as follows: during progression, PZC eventually invaded the surrounding components and grew spherically irrespective of anatomical limitations, resulting in a tendency to a lower ΔTA/MTA. Furthermore, there is a substantially varied distribution of ΔTA/MTA values in cases with a small MTV, particularly those with a MTV of <1 mL. In these cases, the tumour volume is so small that tumours tend to extend irrespective of the shape of PZ. However, the shapes of MTA are not always circular, despite the lack of anatomical limitation for extending until they grow inot large tumours.

We then assessed the association between ΔTA/MTA and several clinicopathological factors. Of these, ECE, SMS and PNI were identified as significant and closely related to ΔTA/MTA. Collectively, these findings suggest that ΔTA/MTA, which represents the extension pattern of PZC along the anatomical shape of the PZ, could be used as a novel factor reflecting the degree of PZC extension.

We determined whether ΔTA/MTA had an effect on the prognosis of patients with PZC undergoing RP. Multivariate analysis using the Cox proportional hazards model identified ΔTA/MTA in addition to several conventional factors, including preoperative serum PSA level, ECE, SVI and SMS, as independent predictors of biochemical recurrence after RP. There was a significant difference in biochemical recurrence-free survival in the 128 patients according to their ΔTA/MTA value. Considering these findings, the degree of disease extension along the anatomical shape of the PZ quantified by ΔTA/MTA could be used to predict the biochemical outcome after RP.

There are several limitations to the present study. To draw definitive conclusions it would be necessary to undertake prospective studies with more patients and with a longer follow-up. In addition, this study analysed the extension patterns of PZC alone; therefore, the significance of ΔTA/MTA in TZC remains unknown. However, considering the progression patterns of TZC growing spherically in the TZ [10], it might be necessary to introduce other variables representing the extension pattern of TZC. Finally, with respect to the time required for calculating ΔTA/MTA, routine use of this variable for pathological examination could not always be recommended; hence, the introduction of a simpler variable than ΔTA/MTA would be expected.

In conclusion, the present findings suggest that PZC extends along the anatomical shape of the PZ during the process of extension in the prostate gland, and that the extension pattern of PZC can be closely represented by the ΔTA/MTA value. Despite the need for further studies, ΔTA/MTA, which is significantly associated with certain kinds of adverse pathological factors, could be used as an independent indicator of biochemical outcome in patients undergoing RP.

CONFLICT OF INTEREST

None declared.

REFERENCES

1 **McNeal JE.** Regional morphology and pathology of the prostate. *Am J Clin Pathol* 1968; **49**: 347–57
2 **Augustin H, Erbersdobler A, Graefen M *et al.*** Biochemical recurrence following radical prostatectomy: a comparison between prostate cancers located in different anatomical zones. *Prostate* 2003; **55**: 48–54
3 **Van de Voorde WM, Van Poppel HP, Verbeken EK, Oyen RH, Baert LV, Lauweryns JM.** Morphological and neuroendocrine features of adenocarcinoma arising in the transition zone and in the peripheral zone of the prostate. *Mod Pathol* 1995; **8**: 591–8
4 **Noguchi M, Stamey TA, McNeal JE, Yemoto CE.** An analysis of 148 consecutive transition zone cancers: clinical and histological characteristics. *J Urol* 2000; **163**: 1751–5
5 **McNeal JE, Redwine EA, Freiha FS, Stamey TA.** Zonal distribution of prostatic adenocarcinoma: correlation with histologic pattern and direction of spread. *Am J Surg Pathol* 1998; **12**: 897–906
6 **Erbersdobler A, Fritz H, Schnöger S *et al.*** Tumor grade, proliferation, apoptosis, microvessel density, p53, and bcl-2 in prostate cancers: differences between tumors located in the transition zone and in the peripheral zone. *Eur Urol* 2002; **41**: 40–6
7 **Sakai I, Harada K, Hara I, Eto H, Miyake H.** A comparison of the biological features between prostate cancers arising in the transition and peripheral zones. *BJU Int* 2005; **96**: 528–32
8 **Miyake H, Sakai I, Ishimura T, Hara I, Eto H.** Significance of cancer detection in the anterior lateral horn on systematic prostate biopsy: the effect on pathological findings of radical prostatectomy specimens. *BJU Int* 2004; **93**: 57–9
9 **Walsh PC.** Radical prostatectomy: a

procedure in evolution. *Semin Oncol* 1994; **21**: 662–71

10 **Greene DR, Wheeler TM, Egawa S, Dunn JK, Scardino PT.** A comparison of the morphological features of cancer arising in the transition zone and in the peripheral zone of the prostate. *J Urol* 1991; **146**: 1069–76

Correspondence: Hideaki Miyake, Division of Urology, Kobe University Graduate School of Medicine, 7-5-1 Kusunoki-cho, Chuo-ku, Kobe 650-0017, Japan.
e-mail: hideakimiyake@hotmail.com

Abbreviations: **RP**, radical prostatectomy; **(M)TA**, (maximum) tumour area; **MTV**, maximum tumour volume; **PZ(C)**, peripheral zone (cancer); **TZ(C)**, transitional zone (cancer); **ECE**, extracapsular extension; **SVI**, seminal vesicle invasion; **PNI**, perineural invasion; **SMS**, surgical margin status.

The bcl2 −938CC Genotype Has Poor Prognosis and Lower Survival in Renal Cancer

Hiroshi Hirata, Yuji Hinoda, Koichi Nakajima, Nobuyuki Kikuno, Yutaka Suehiro, Z. Laura Tabatabai, Nobuhisa Ishii and Rajvir Dahiya*

From the Departments of Urology (HH, NK, RD) and Pathology (ZLT), San Francisco Veterans Affairs Medical Center and University of California-San Francisco, San Francisco, California, and Department of Oncology and Laboratory Medicine, Yamaguchi University Graduate School of Medicine (YH, YS), Yamaguchi and Department of Urology, Toho University Faculty of Medicine (KN, NI), Tokyo, Japan

Purpose: A single nucleotide polymorphism (−938C/A, rs2279115) was found in the *bcl2* gene, whose −938A allele is significantly associated with increased Bcl2 expression compared with that of the C allele. Bcl2 up-regulation was reported to be associated with longer survival in patients with renal cancer. However, to our knowledge there is currently no information on the role of the *bcl2*-938C/A single nucleotide polymorphism in renal cell carcinoma cases. Therefore, we investigated the polymorphism at the *bcl2* −938C/A site and its effects on clinical characteristics in patients with renal cell carcinoma.

Materials and Methods: We genotyped the *bcl2*-938C/A single nucleotide polymorphism in 216 patients with renal cancer, and in 209 healthy age and gender matched controls. We also investigated the relationship between the *bcl2* −938C/A polymorphism, Bcl2 expression, proliferation and apoptosis status in renal cell carcinoma tissues using immunohistochemistry and TUNEL assay. The association of the *bcl2* −938C/A single nucleotide polymorphism with survival in patients with renal cell carcinoma was also analyzed by Kaplan-Meier curves.

Results: Survival in Bcl2 positive cases was significantly longer than in negative cases. On univariate and multivariate analyses the *bcl2* −938CC genotype was independently associated with poor prognosis. Kaplan-Meier analysis showed that survival in patients with CC genotypes was significantly worse than in those with CA+AA genotypes. CC genotype carriers had significantly lower Bcl2 expression and higher proliferative activity in renal cancer tissues than CA+AA genotype carriers.

Conclusions: To our knowledge this is the first report to show that the *bcl2* −938C/C genotype has worse prognosis and lower survival in patients with renal cell carcinoma. In addition, the *bcl2* −938C/A single nucleotide polymorphism was shown to be an independent adverse prognostic factor for renal cell carcinoma.

Abbreviations and Acronyms

Bcl2 = B-cell lymphoma
IHC = immunohistochemistry
PCR = polymerase chain reaction
PI = proliferation index
RCC = renal cell carcinoma
RFLP = restriction fragment length polymorphism
SNP = single nucleotide polymorphism

Submitted for publication October 31, 2008.

Study received Shimane Medical University and Toho University approval.

Supported by National Institutes of Health Grants RO1CA101844, R01CA111470 and T32-DK07790, a Veterans Affairs REAP award, Merit Review grants and the Yamada Science Foundation.

* Correspondence: Urology Research Center (112F), Veterans Affairs Medical Center and University of California-San Francisco, 4150 Clement St., San Francisco, California 94121 (telephone: 415-750-6964; FAX: 415-750-6639; e-mail: rdahiya@urology.ucsf.edu).

Key Words: kidney; carcinoma, renal cell; polymorphism, single nucleotide; apoptosis; genotype

AMONG urological tumors RCC is the third leading cause of death, accounting for about 2% of adult malignancies.[1] Although the detection rate of RCC has increased with improved diagnostic techniques, metastatic lesions are still found at diagnosis in about 25% of patients with RCC. Moreover, in patients with RCC distant metastasis is sometimes found

0022-5347/09/1822-0721/0
THE JOURNAL OF UROLOGY®

Vol. 182, 721-727, August 2009
Printed in U.S.A.
DOI:10.1016/j.juro.2009.03.081

long after surgical removal of the primary tumor. After detecting these metastases the 5-year survival rate is generally less than 10%.[2] Standard treatment for localized renal cancer is surgical removal, while immunotherapy is used for metastatic disease because of its multidrug resistance. Interleukin-2 was the most common immunotherapy for RCC but it was effective in only 10% to 15% of patients.[2,3] Recently targeted tyrosine kinase inhibitors have been used for advanced RCC with improved progression-free and overall survival compared with that of interferon treatment.[4]

Bcl2 family proteins, which are well-known as mitochondrial membrane proteins, are important regulators of programmed cell death or apoptosis in normal tissues and cancer cells.[5] Bcl2 family proteins contain anti-apoptotic proteins such as Bcl2 and Bcl-xL, and pro-apoptotic proteins such as Bax and Bak.[5] High Bcl2 expression is associated with poor survival in several different cancers, including B-cell chronic lymphocytic leukemia, prostate cancer and urinary tract transitional cell cancer.[6–8] In contrast, Bcl2 up-regulation is associated with longer survival in various cancers, including colon, breast and nonsmall cell lung cancer.[9–12] In RCC cases previous studies have shown an association between increased Bcl2 expression and better prognosis.[13,14]

The *bcl2* gene, which is located on chromosome 18q21.3, consists of 3 exons and the 2 promoters P1 and P2.[13] Interestingly these promoters have different functions. P2, located 1400 bp upstream of the translation initiation site, decreases the activity of P1 promoter function.[15]

A novel functional single nucleotide polymorphism (−938C/A, rs2279115) was found in the P2 negative regulatory element. The −938C allele was significantly associated with increased P2 promoter activity and binding of nuclear proteins compared with the A allele, resulting in overall decreased bcl2 promoter transcriptional activity.[16] Bcl2 protein expression in patients with chronic lymphocytic leukemia who carry the –938C/C genotype is significantly decreased compared to that in patients with the –938A/A genotype.[16]

Therefore, due to this evidence we hypothesized that 1) the *bcl2* promoter −938C/A polymorphism may increase Bcl2 expression in renal cancer tissues, 2) increased Bcl2 expression may be associated with longer survival in patients with RCC and 3) the *bcl2* −938C/A polymorphism may be an important prognostic indicator in patients with RCC. To test these hypotheses we performed a case-control study genotyping the polymorphic site in *bcl2* −938C/A. We also investigated the relationship between Bcl2 expression in RCC tissues and genotypes with the *bcl2* −938C/A polymorphism. In addition, we examined the relationship between the *bcl2* −938C/A polymorphism and apoptosis/proliferation status in RCC tissues using the TUNEL assay and Ki-67 IHC.

MATERIALS AND METHODS

Samples

Genomic DNA was extracted from peripheral blood in 160 patients and from paraffin embedded noncancerous kidney tissue in 56 as well as from 209 healthy individuals. A DNA mini kit (QIAgen®) was used to extract DNA from normal tissue and peripheral blood according to manufacturer protocols. A total of 149 male and 67 female patients with pathologically confirmed conventional RCC, and 209 age and sex matched controls were enrolled in this study. Mean age in patients and controls was 62.2 and 61.6 years, respectively (ANOVA p = 0.62, table 1). All 216 patients tested were diagnosed with RCC based on histopathological findings. Disease was classified according to WHO criteria and staged according to the TNM classification. Healthy controls consisted of volunteers with no apparent abnormal findings upon medical examination at Shimane University Hospital. Peripheral blood samples were obtained from patients and controls after written informed consent was obtained at Shimane University Hospital and Toho University Hospital. This study was approved by Shimane Medical University and Toho University. Study samples were previously reported.[17]

Genotyping

Polymorphisms were analyzed by PCR-RFLP. The PCR primers used for *bcl2* were GCGTCCTGCCTTCATTTATC

Table 1. *Characteristics of patients with RCC and controls*

	No. Pts	No. Controls (%)
Overall	216	209
Mean ± SD age*	62.2 ± 12	61.6 ± 14
Gender:†		
M	149 (69)	149 (71)
F	67 (31)	60 (29)
Grade:		
1	52 (24.1)	
2	137 (63.4)	
3 + 4	27 (12.5)	
pT:		
1	117 (54.2)	
2	46 (21.3)	
3	50 (23.1)	
4	3 (1.4)	
pN:		
Neg	199 (92.1)	
Pos	17 (7.9)	
pM:		
Neg	192 (88.9)	
Pos	24 (11.1)	
Pathological findings:		
Clear cell Ca	203 (94.0)	
Granular cell Ca	11 (5.1)	
Chromophobe cell Ca	2 (0.9)	

* p = 0.62.
† p = 0.55.

(bcl2 first forward), TTCCAGATCGATTCCCAGAC (bcl2 first reverse), CGTCCTGCCTTCATTTATCC (bcl2 second forward) and TTCGCAGAAGTCCTGTGATG (bcl2 second reverse). PCR reactions were done in a total volume of 20 μl consisting of 0.3 μl 10 μmol/l solution of each primer, 1.5 mmol/l $MgCl_2$, 0.8 mmol/l deoxynucleotide triphosphate, 0.5 U REDTaq® DNA polymerase, 1 μl (80 ng/μl) genomic DNA and 15.6 μl H_2O using a PTC 200 Thermal Cycler (MJ Research, Waltham, Massachusetts). All reactions were subjected to 2 amplification rounds using a nested primer approach. The first and second PCR annealing temperatures and PCR cycles were 52C and 48 cycles, and 58C and 45 cycles, respectively. The second PCR products (195 bp), including the polymorphic site, were digested with the restriction enzyme *BccI* (New England BioLabs®) at 37C for 3 hours, separated on 2.0% agarose gel and stained with ethidium bromide. Unrestricted products (195 bp) represented the C/C genotype and restricted products (74 and 121 bp) represented the A/A genotype. To confirm the genotype found on PCR–RFLP approximately 50% of PCR sample products were randomly selected and subjected to direct sequencing using an ABI PRISM® 377 DNA sequencer.

IHC Study

Immunostaining of Bcl2 and Ki67 was performed on 56 formalin fixed, paraffin embedded renal cancer specimens. Anti –Bcl2 and anti-Ki67 antibodies (sc509, sc23900; Santa Cruz Biotechnology, Santa Cruz, CA) were used and the staining procedure was performed according to a commercial kit (Santa Cruz Biotechnology). The sections were counterstained with Harris hematoxylin. A pathologist evaluated the immunostaining while blinded. IHC staining was evaluated by assessing staining intensity on a scale of 0 to 3 using a microscope at 200×. All specimens were scored blindly by 2 observers. Expression intensity was scored as 0—negative, 1+—weakly positive, 2+—moderately positive and 3+—strongly positive with high expression considered a score of 2 and 3 (2 + 3/[0 + 1 + 2 + 3] × 100%).

Apoptosis and Proliferation

To detect apoptosis in renal cancer cells we used the TUNEL assay with an Apo-BrdU-IHC in situ DNA fragmentation assay kit (BioVision, Mountain View, California) according to manufacturer instruction. Apoptotic cell nuclei stained brown and nonapoptotic nuclei stained green. Apoptotic and total nuclei were counted in 10 fields at 100× magnification. The apoptotic index is expressed as the percent of apoptotic cells of the total number of cells in the given area. Ki-67 positive nuclei were counted in 10 fields at 100× magnification. The PI is expressed as the percent of Ki-67 positive cells of the total number of cells in the given area. Apoptosis and proliferation assessment was performed by a pathologist in blinded fashion.

Statistical Analysis

Hardy-Weinberg equilibrium was evaluated by SNPAlyze™, version 2.2 using an expectation maximization method. ANOVA and the chi-square test were used to compare clinical characteristics and genotype frequency between patients and controls. The OR was determined by unconditional logistic regression analysis and adjusted for age as a continuous variable. All statistical analyses were performed using StatView™, version 5 with $p < 0.01$ considered statistically significant. Genotype frequencies of the polymorphisms in 209 control and 216 case samples did not deviate from Hardy-Weinberg equilibrium ($p > 0.05$).

RESULTS

Patients With RCC and Controls

Characteristics. Table 1 shows mean age, gender, tumor grade and pathological findings in patients with RCC. The 2-tailed Student's t test and ANOVA were used to compare age and gender distributions between patients and controls. Of 216 RCC cases disease was localized in 163 (75.5%), grade 1 and 2 in 189 (87.5%), and the clear cell type in 203 (94.0%).

Genotype distribution and effect on clinical factors. Tables 2 and 3 list demographic and clinicopathological characteristics, including tumor grade and pathological TNM classification, in all RCC cases based on *bcl2* –938C/A genotypes. Genotype distribution and allele frequency in patients with RCC were not significantly different from those in controls (table 2). There was no positive correlation between *bcl2* –938C/A polymorphism and clinicopathological factors (table 2). Figure 1 shows a typical RFLP gel and sequencing.

Bcl-2 Expression and Genotype

To investigate the correlation between *bcl2* gene polymorphism (rs2279115) and Bcl2 protein expression IHC was done in 56 genotyped renal cancer tissues (fig. 2). Two of 56 formalin fixed, paraffin embedded renal cancer specimens were not clear cell carcinoma. Therefore, we assessed 54 clear cell carcinoma samples. We noted the expression level of Bcl2 in each genotype of the *bcl2* –938 C/A polymorphism. Figure 2, *A* shows the rate of Bcl2 expression in each genotype. The expression rate of AA, CA and CC genotypes was 80% (8 of 10 preparations), 52% (11 of 21) and 30% (7 of 23), respectively (fig. 2, *A*). Bcl2 expression was significantly lower in *bcl2* C/C genotype carriers (fig. 2, *A*). Bcl2 positive cells had brown stained cytoplasm. Figure 2, *B* shows representative Bcl2 expression.

Table 2. *Bcl2 genotype in patients with RCC and controls*

Bcl2-938C/A Genotype	No. Pts (%)	No. Controls (%)	p Value
Overall	216	209	
A/A	41 (19.0)	36 (17.2)	Referent
C/A	83 (38.4)	72 (34.4)	0.96
C/C	92 (42.6)	101 (48.3)	0.41
C/A+C/C	175 (81.0)	173 (82.8)	0.64

Table 3. *Demographic and clinicopathological characteristics, and bcl2 genotype in patients with RCC*

	No. Genotype				
	A/A	C/A	C/C	C/A + C/C	Total No.
Gender:					
F	13	31	23	54	67
M	28	52	69	121	149
p Value	Referent	0.53	0.42	0.92	
Grade:					
1 + 2	33	76	80	156	189
3 + 4	8	7	12	19	53
p Value	Referent	0.07	0.34	0.13	
pT:					
pT1 + pT2	30	68	65	133	163
pT3 + pT4	11	15	27	42	53
p Value	Referent	0.26	0.76	0.71	
pN:					
Neg	37	80	82	162	199
Pos	4	3	10	13	17
p Value	Referent	0.16	0.84	0.62	
pM:					
Neg	37	74	81	155	192
Pos	4	9	11	20	24
p Value	Referent	0.85	0.71	0.76	

IHC Results and Clinical Prognosis

Using Bcl2 IHC expression results overall survival was analyzed by the Kaplan-Meier method. Survival in Bcl2 positive cases was significantly longer than in negative cases (p = 0.0386, fig. 3).

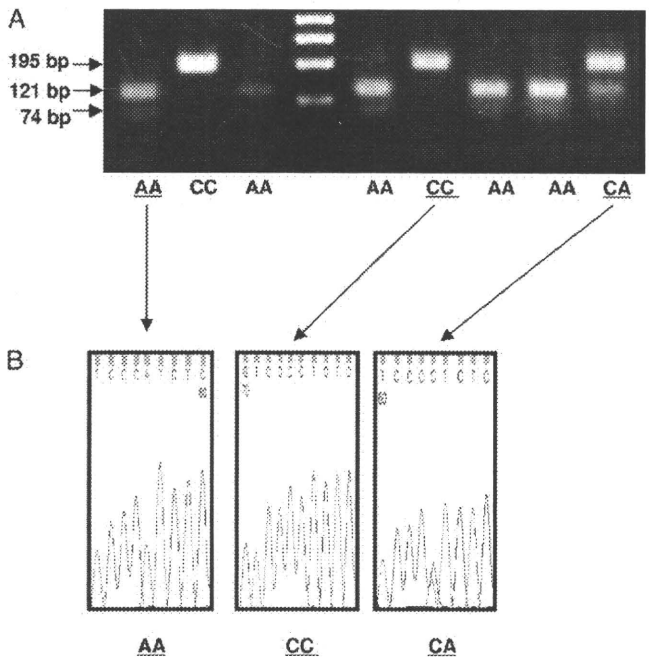

Figure 1. *A, bcl2* −938C/A polymorphism RFLP gels. Unrestricted 195 bp products represent C/C genotype, and restricted 74 and 121 bp products represent A/A genotype. *B,* DNA sequencing.

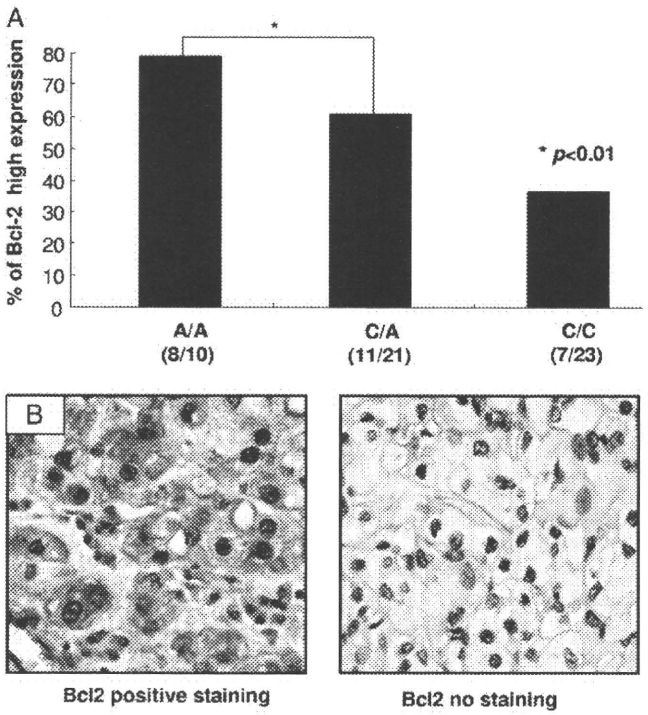

Figure 2. *A,* correlation between *bcl2* −938 C/A genotypes and Bcl2 expression. Asterisk indicates *bcl2* C/C vs other genotypes p value. *B,* representative Bcl-2 immunostaining in renal cancer. Reduced from ×200.

Apoptosis, Proliferation and *bcl2* Genotype

To investigate the correlation between *bcl2* gene polymorphism (rs2279115) and apoptosis the TUNEL assay was done in 54 genotyped renal cancer tissues. The apoptotic index was significantly higher in *bcl2* C/C carriers than in C/A and A/A carriers (median

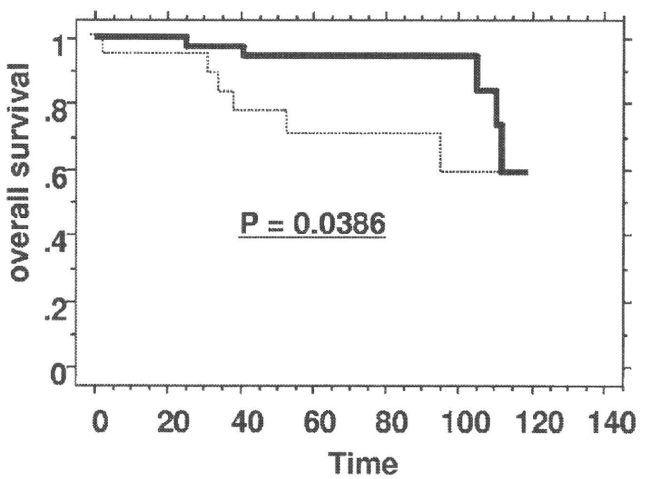

Figure 3. Overall survival based on Kaplan-Meier curves and Bcl2 expression on IHC in 56 patients with RCC. Bold line represents Bcl2 HIC positive in 38 patients. Dashed line indicates Bclt IHC negative in 18 patients.

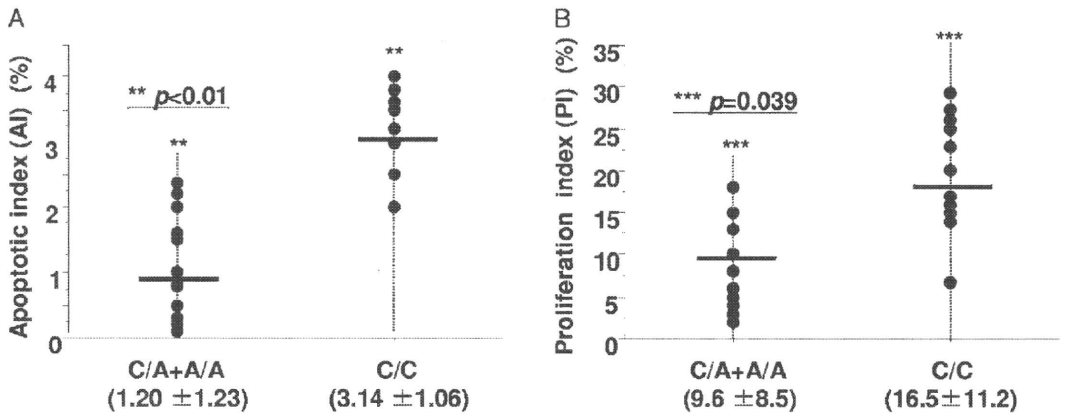

Figure 4. Genotyped RCC tissue *bcl2* –938C/A polymorphism. *A*, apoptosis. *B*, proliferation. Horizontal bars indicate mean. X axis indicates *bcl2* SNP genotype.

3.14 vs 1.20) (fig. 4, *A*). PI was also measured in the 54 genotyped RCC tissues. Similar to apoptosis results, PI was significantly higher in *bcl2* C/C carriers than in C/A or A/A carriers (median 16.5 vs 9.6) (fig. 4, *B*).

Cox Proportional Hazard Analysis of Overall Survival

The prognostic value of overall survival using parameters such as gender, age at diagnosis, pathological subtype, tumor grade, pTNM and *bcl2* SNP were analyzed using Cox proportional hazards analysis (table 4). On univariate analysis tumor grade, pT, pN, pM and *bcl2* SNP were associated with survival (table 4 and fig. 5). On multivariate analysis *bcl2* SNP and pTNM were independent risk factors for overall survival.

DISCUSSION

To our knowledge we report for the first time that the *bcl2 –938C/C* genotype is associated with a poor outcome in patients with RCC. On univariate analysis tumor grade, pTNM and *bcl2* SNP were statistically significant prognostic factors. In addition, multivariate Cox proportional hazard analysis revealed that this polymorphism could be an independent prognostic factor. Thus, we found a significant effect of the *bcl2* –938 C/A polymorphism on overall survival in patients with RCC.

Various groups have indicated the prognostic role of Bcl2 expression in various kinds of cancer and the effect of Bcl2 expression on prognosis is different among cancers.[6–14] In some cancers, such as breast, colon, kidney and nonsmall cell lung cancer, increased Bcl2 expression is associated with good prognosis, while there is an inverse association in other types.[6–14] In regard to RCC Itoi et al reported that Bcl2 expression significantly correlates with better survival.[14] Kallio et al reported that Bcl2 expression is associated with better prognosis in patients with RCC.[13] In our study there was a more favorable prognosis in Bcl2 positive vs negative cases, consistent with previous reports.[13,14]

To our knowledge there are no reports of the *bcl2* –938C/A polymorphism as a risk factor for renal cancer. Therefore, we analyzed the *bcl2* –938C/A polymorphism and Bcl2 expression in RCC tissues. We found that Bcl2 protein expression in RCC tissues was higher for the C/A+A/A genotype than for the C/C genotype. In patients with chronic lympho-

Table 4. *Univariate and multivariate Cox proportional hazard analysis of death risk in patients with RCC*

Parameter	Univariate		Multivariate	
	HR (95% CI)	p Value	HR (95% CI)	p Value
Gender (M vs F)	0.97 (0.43–2.18)	0.94		
Age at diagnosis (younger than 61 vs 61 or older)	1.84 (0.78–4.36)	0.16		
Pathological findings (clear cell Ca vs other)	1.61 (0.34–7.59)	0.54		
Grade (G2+G3+G4 vs G1)	2.3 (1.12–4.35)	0.03	1.4 (0.21–4.78)	0.77
pT (pT3+pT4 vs pT1+pT2)	4.87 (2.14–11.12)	0.0002	2.49 (1.25–5.05)	0.02
pN (pN1/pN2 vs pN0)	11.55 (2.24–59.53)	0.003	9.31 (1.36–63.65)	0.03
pM (pM1 vs pM0)	26.66 (5.50–129.12)	<0.0001	26.66 (4.40–129.21)	0.0002
Bcl2 SNP (rs2279115) (CC vs CA+AA)	2.4 (1.11–5.18)	0.026	2.16 (1.01–6.45)	0.048

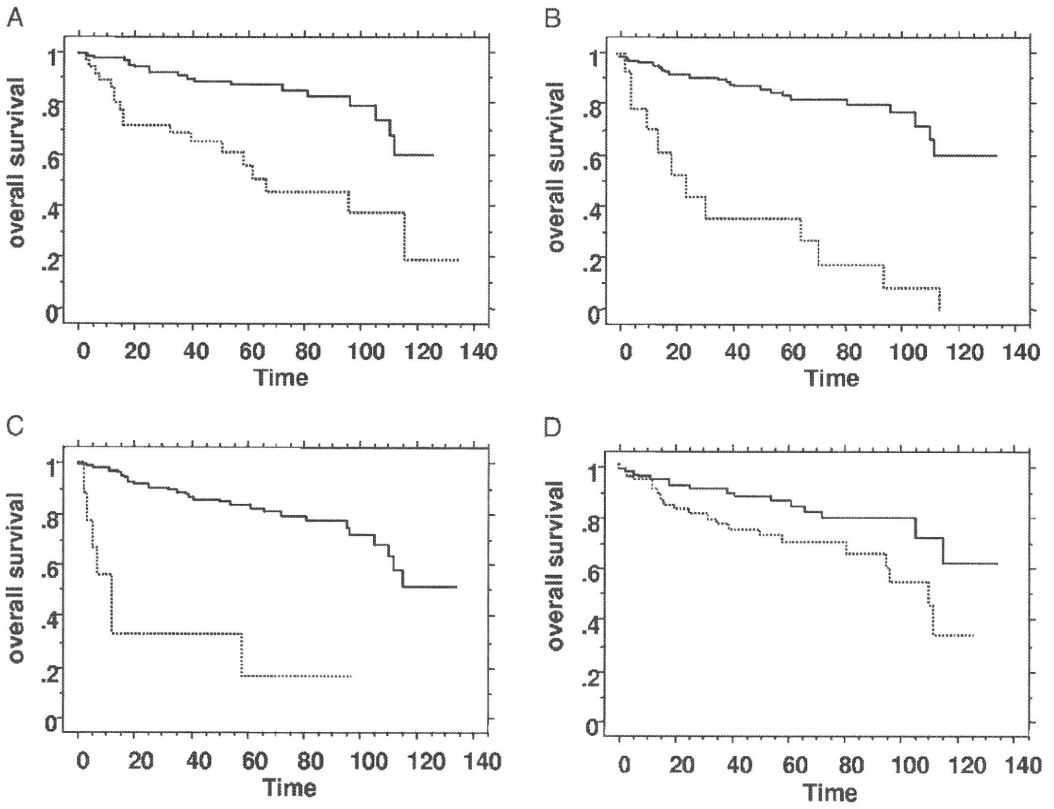

Figure 5. Overall survival based on Kaplan-Meier curves in 176 patients with RCC. *A*, tumor stage pT3/pT4 was independent predictor of overall survival ($p < 0.0001$). Solid line indicates pT1 and pT2. Dashed line indicates pT3 and pT4. *B*, distant metastasis was independent predictor of overall survival ($p < 0.0001$). Solid line indicates pM0. Dashed line indicates pM+. *C*, lymph node metastasis was independent predictor of overall survival ($p < 0.0001$). Solid line indicates pN0. Dashed line indicates pN+. *D*, *bcl2* C/C genotype was independent predictor of overall survival ($p = 0.0061$). Survival in C/C carriers (dashed line) was statistically significantly worse than in C/A+A/A carriers (solid line).

cytic leukemia and breast cancer the effect of the *bcl2* −938C/A polymorphism on survival is inconsistent, although Bcl2 protein expression in tissue from those with −938A/A genotypes was consistently increased compared with expression in those with the C/C genotype.[16,18] Our current results agree with these findings, namely that the *bcl2* −938A allele is tightly linked to increased Bcl2 expression.

The Bcl-2 family has an important role in apoptosis regulation and cell proliferation inhibition.[5] However, the data are mixed as to the relationship between Bcl2 expression and apoptosis or cell proliferation in cancer tissue. For instance, Sinicrope et al found that high Bcl2 protein levels significantly correlated with low proliferative activity in colon cancer cases.[19] However, others reported that Bcl2 expression is inversely associated with proliferative activity in nonHodgkin's lymphoma cases.[18] Similarly in RCC mixed results have been reported.[13,14,20] However, to our knowledge there has been no study to date of a correlation between the *bcl2* −938C/A polymorphism and RCC apoptosis or proliferation. Therefore, we compared apoptosis and cell proliferation with the *bcl2* −938C/A polymorphism using genotyped RCC tissue samples. These results show significantly higher TUNEL positive cells and proliferative cells in *bcl2* −938C/C carriers than in C/A+A/A carriers. These data suggest that the *bcl2* −938C/C genotype is associated with lower Bcl2 expression and higher cell proliferation in RCC cases. Previous reports have shown the relationship between Bcl2 expression and its inhibitory effect on cell proliferation in renal cancer, which supports our present data.[14,21] To our knowledge the molecular mechanisms of how Bcl2 is involved in carcinogenesis inhibition remain unknown. However, Bcl2 was described to be associated with cell cycle inhibition.[22] In an in vivo study increased Bcl2 expression delayed cell cycle entry and decreased cell proliferation.[22]

Since Bcl2 is an efficient inhibitor of drug induced apoptosis, it is important for renal cancer since almost no chemotherapy drugs are effective for RCC. Recently targeted tyrosine kinase inhibitors are used in advanced RCC cases[4] and numerous genes are thought to affect the success or failure of cancer chemotherapy.[23,24] Several mechanisms contribute